# Carbon Nanotubes: Properties and Functionalization

David E. Luzzi
Department of Materials Science
University of Pennsylvania
Philadelphia, PA 19104

**Carbon Nanotubes**
**Properties and Functionalization**

David E. Luzzi
Department of Materials Science and Engineering
University of Pennsylvania
Philadelphia, PA 19104

# Carbon Nanotubes
# Properties and Functionalization

David E. Luzzi
University of Pennsylvania

Training Workshop on Nano-Biotechnology
NASA Langley Research Center, June 14-15, 2000

## Introduction

- Nanoscale Hybrid Materials
- Chemistry in Confined Environments
- Single Molecule/Single Atom Detection

## Allotropes of Carbon

The different allotropes of carbon by class. Clockwise from upper left. Diamond, $C_{60}$, representing the many fullerene closed cage structures formed from mixtures of five and six member carbon rings, (10,10) nanotube, representing the many nanotube structures, achiral and chiral formed by wrapping a single, or multiple nested graphene sheets into a tube, graphite. This figure is from the Rice University web page of Rick Smalley.

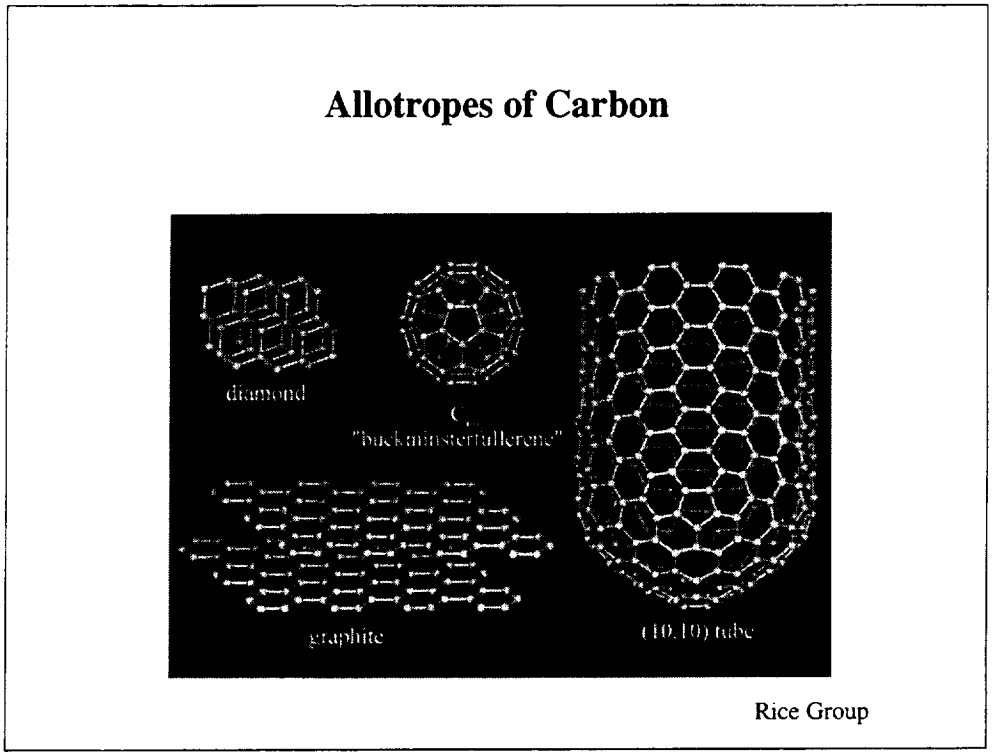

## Production of Nanotubes

A complete summary (as of the time of the workshop) of the methods used to produce nanotubes with the year of publication and responsible organization listed. The list is confined to those methods for which rigorous evidence of the existence of closed tubes of graphene sheets extending over long distances has been presented, usually via transmission of electron microscope (TEM) images.

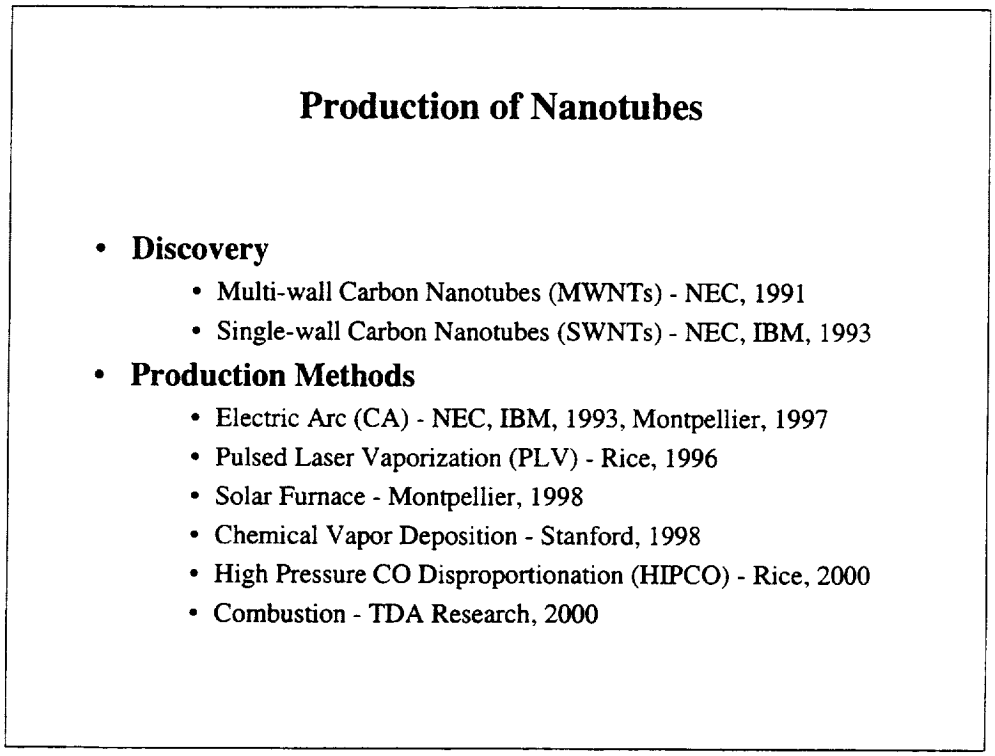

## Aligned Single-Wall Carbon Nanotubes

Carbon nanotubes have been aligned by three methods: under high magnetic fields; by melt spinning within a polymer matrix; and under the influence of an electric field. The micrograph is of tubes@rice material (PLV method) aligned with a 25T magnetic field (Rice group). Measurement of the FWHM alignment was done using electron diffraction (Penn).

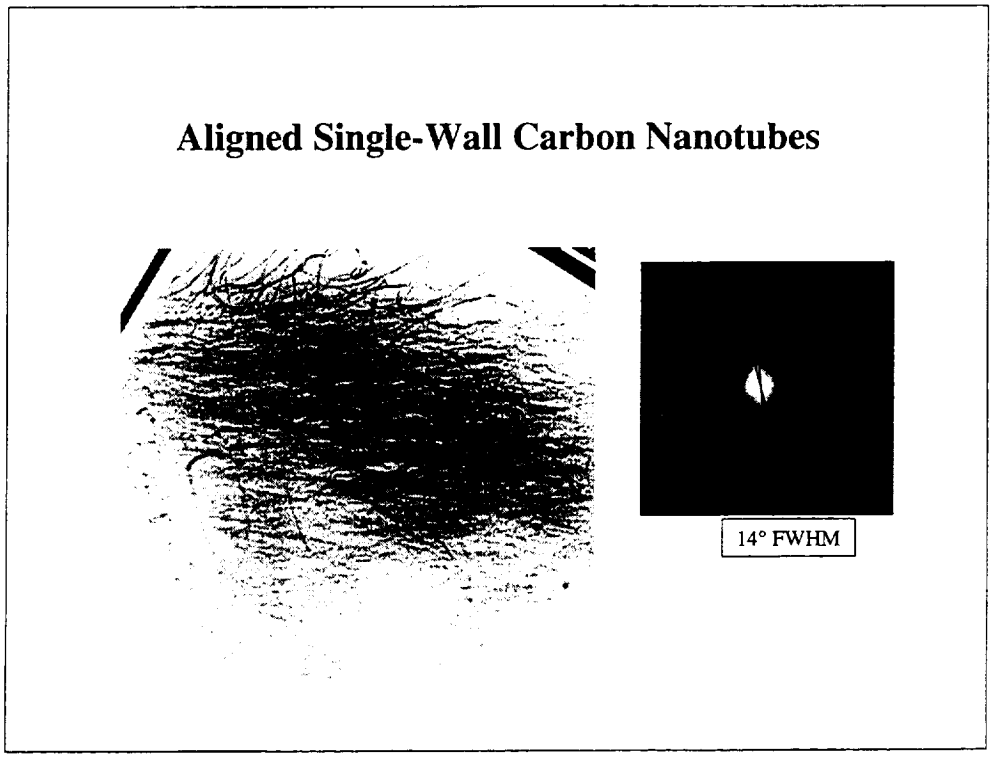

## EM of a Nanotube
## (10, 10) SWNT

A high magnification image of a single-wall carbon nanotube (SWCNT) compared to a schematic. In the phase imaging condition, all scattered and unscattered electrons that pass through the lens pole pieces are used to produce the image. Due to its low atomic number, carbon scatters electrons weakly. Under phase imaging conditions, nanotubes can, therefore, be considered as weak phase objects. Images of weak phase objects will be two-dimensional projections along the electron beam direction of the three dimensional specimen potential convoluted with the point transfer function of the electron microscope. With the resolution of the microscope significantly better than the finest scale detail in an image, the image can be considered to be a direct magnification of the carbon shells. The intra-shell structure of the modified graphene sheet is below the resolution limit of the microscope and appears as a uniform contrast level (gray). Since the maximum scattering potential of the nanotube exists where the structure is tangent to the electron beam, the images will appear as a pair of parallel lines.

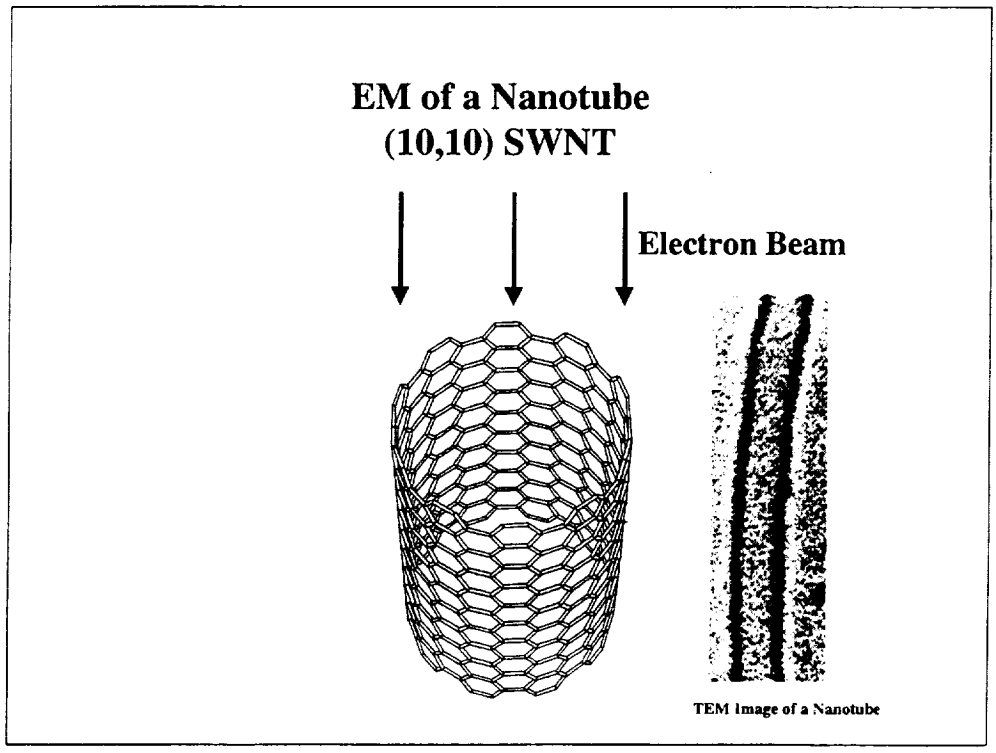

## Cutting Nanotubes to Length

The ideal structure of a carbon nanotube is a perfect closed sheet of hexagonal rings of carbon atoms. Exposure to an oxidizing environment has been shown to damage the nanotube, even producing sizeable holes in the sidewall and opening the ends. It is not known why this process is localized, but the result is useful for certain applications.

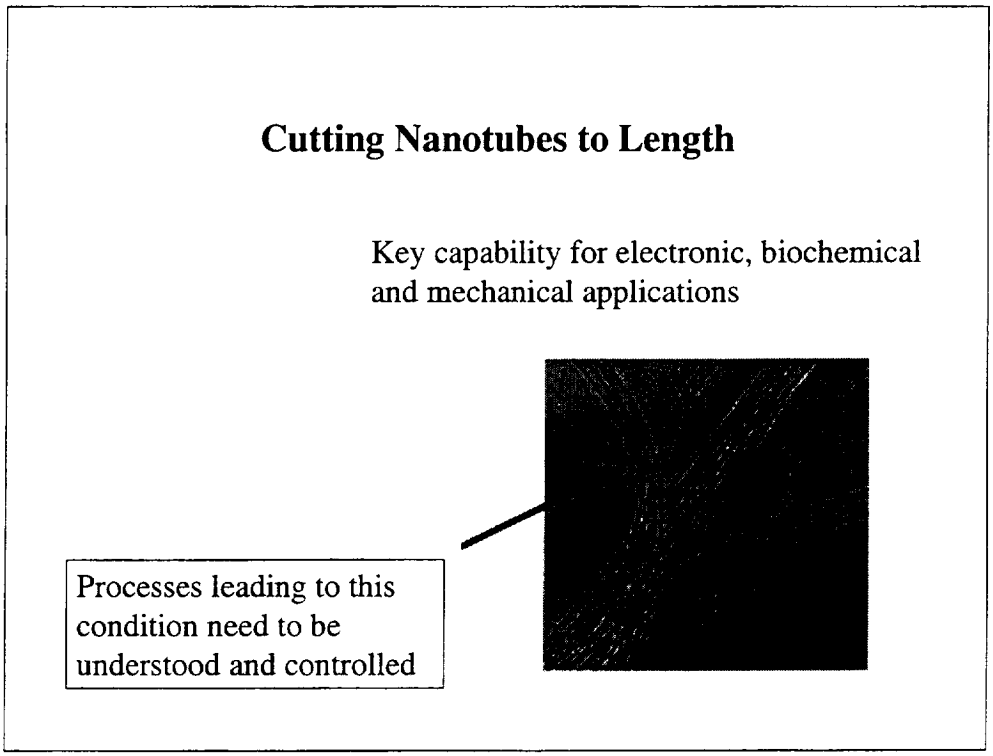

## Thermal and Chemical Stability of Carbon Nanotubes

This is an incomplete summary of the response of nanotubes to some environments – included for guidance only.

### Thermal and Chemical Stability of Carbon Nanotubes

- In vacuum
  - Stable range - from < 90 K to > 1500 K
  - Some reports above 1500 K, but unconfirmed
- In argon
  - Tested range RT to 1200 °C - stable
  - Coalesce at high temperatures
- In air
  - Decompose at ~ 400 °C
- Chemically stable, however
  - Attacked in oxidizing environments
  - Attacked by strong ultrasonic disturbance

## Particle/SWNT Interaction

In order to electron irradiation damage in nanotubes, we can calculate the minimum incident electron energy (e.g., accelerating voltage) required for ballistic ejection of a carbon atom to occur. To facilitate this calculation, we define the primary knock-on atom (PKA) as the carbon atom targeted for displacement. Since a nanotube may adopt any spatial orientation with respect to the electron beam, a complete description of the relevant interaction geometry is required. The PKA is contained by a tangent plane to the nanotube, where **n** is the normal vector to that plane. The vector **r** points along the direction of impulse to the PKA (i.e., the direction of ejection). The vector **b** points along the direction of the incident electron beam. Finally, the angle $\alpha$ is between **n** and **r**, the angle $\gamma$ is between **r** and **b**, and the angle $\delta$ is between **n** and **b** such that $\delta = \alpha + \gamma$. It will be shown that it is only necessary to consider the case where **n**, **r**, and **b** are coplanar. Two factors must be considered in determining whether or not the PKA will be ejected: (1) the energy transferred from the electron beam to the PKA; and (2) the energy barrier that the PKA must overcome to escape from the nanotube. These are embodied in the two terms in the equation, the first governing the energy transfer to the PKA, the second a function fit to discrete tight binding calculations of the anisotropic binding energy of the PKA to the nanotube.

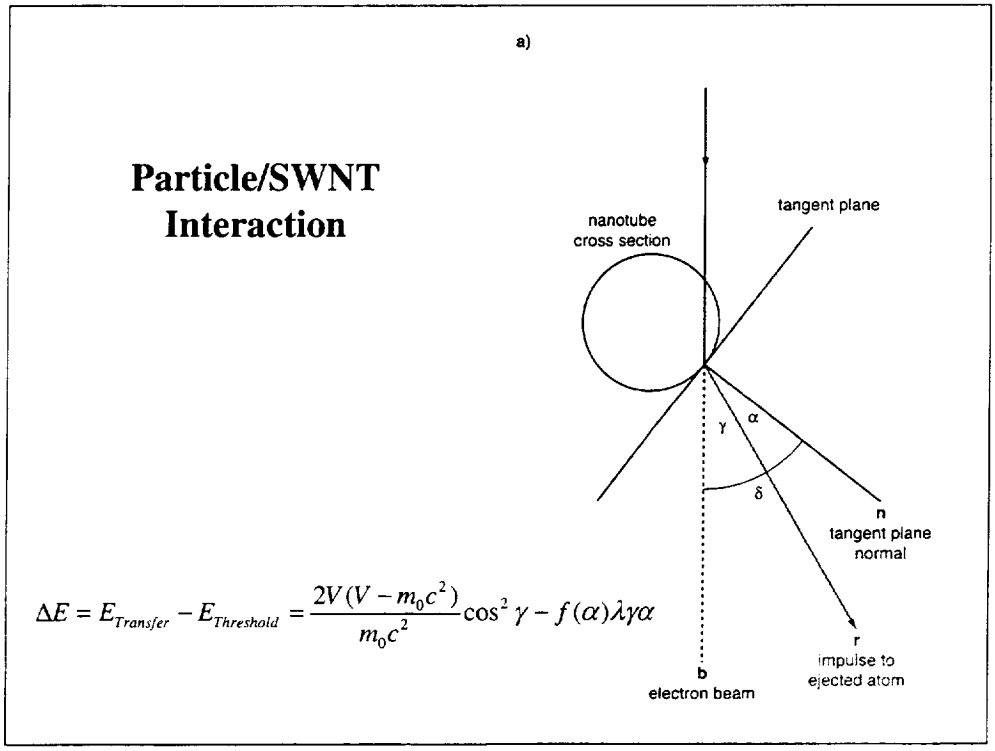

## Geometrical Dependence of Energy Transfer Versus Threshold Energy

At a given incident electron energy (V), at those ($\alpha$, $\gamma$) geometries where $E_{transfer}$ exceeds $E_{escape}$ the PKA will be ejected. These conditions are indicated in the figures which show $\Delta E = E_{transfer} - E_{escape}$ plotted for three different electron energies. For 80 keV electrons, $\Delta E$ is negative for all ($\alpha$, $\gamma$) such that ejection of the PKA is impossible. At 100 keV, $\Delta E$ is positive for a small ($\alpha$, $\gamma$) range such that ejection of the PKA is possible only within a narrow angular spread of both **n** and **b**. Similarly, at 200 keV the energy transfer is sufficiently high that ejection is possible at more severe angles. Note that the cross section for ejection will increase as $\Delta E$ becomes more positive, indicating that ejections are most probable for the geometry ($\alpha$, $\gamma$) = (0, 0). Finally, the threshold energy for knock-on damage occurs where the $\Delta E$ surface has its maximum at 0 eV. This is calculated to occur at an electron energy of 86.4 keV.

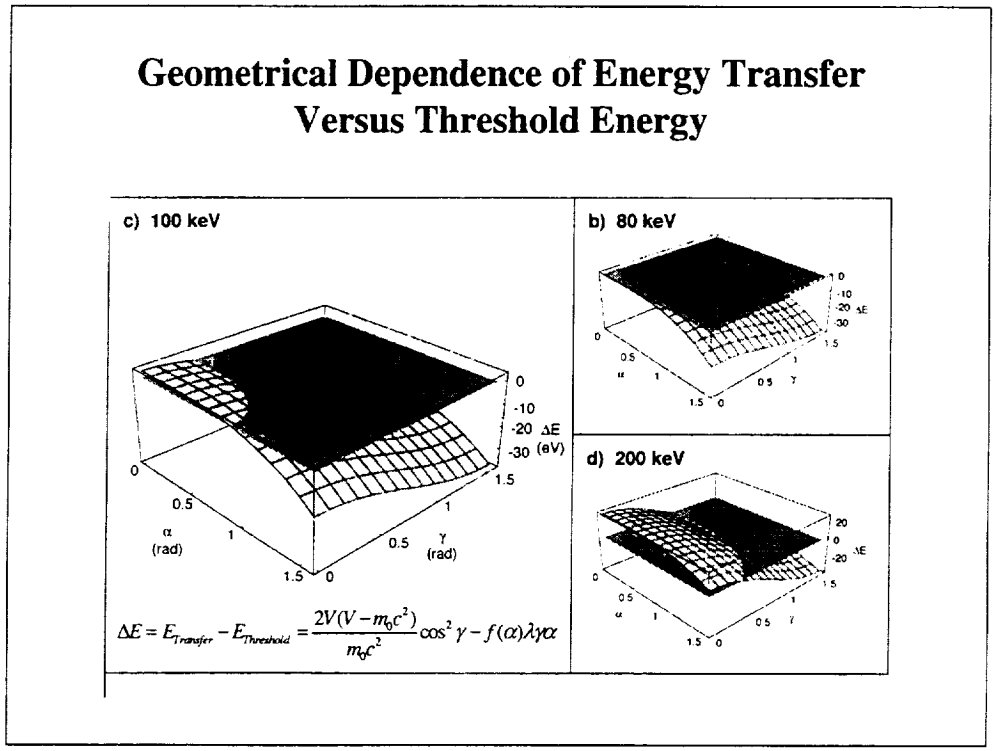

## SWNT Damage Versus Electron Beam Energy

For a known electron beam direction and energy, it is possible to determine which atoms on an SWNT (as defined by their tangent planes) are susceptible to knock-on damage. Consider that the angle $\delta$ can be calculated for each ($\alpha$, $\gamma$) having positive $\Delta E$. The largest $\delta$ for any such ($\alpha$, $\gamma$) occurs when $\alpha$ and $\gamma$ are coplanar. Finally, the $\Delta E$ surface intersects the $\Delta E = 0$ plane along a curve that has the property of giving the largest allowed $\gamma$ for a given $\alpha$, and vice versa. Maximizing the sum $\alpha + \gamma$ along this curve gives the largest possible $\delta$ that can occur for *any* ($\alpha$, $\gamma$) at that beam energy. Any carbon atoms whose tangent plane normals are further from **b** than this angle, which we call $\delta_{max}$, cannot undergo ballistic ejection.

A numerical calculation of $\delta_{max}$ as a function of electron energy is plotted. The corresponding illustration is drawn on the same abscissa as the plot above it and graphically shows which surfaces of a nanotube can be damaged as a function of electron energy for a beam directed down the figure. As before, at 80 keV no carbon atoms can be ejected. At 100 keV, atoms can be ejected for $\delta < 57.5°$, destroying the top and bottom surfaces and leaving only the side walls intact. Above 138.8 keV, all carbon atoms can be ejected.

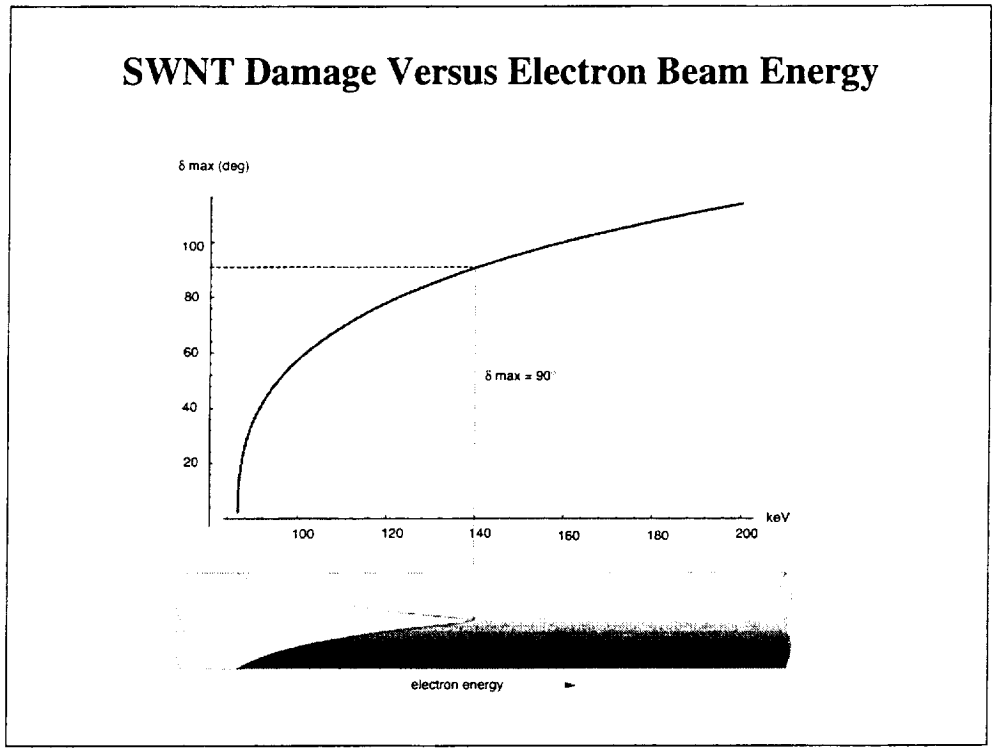

## SWNT Irradiation at 80 keV

At 80 keV, the SWCNT is not damaged by the electron beam even after extensive irradiation.

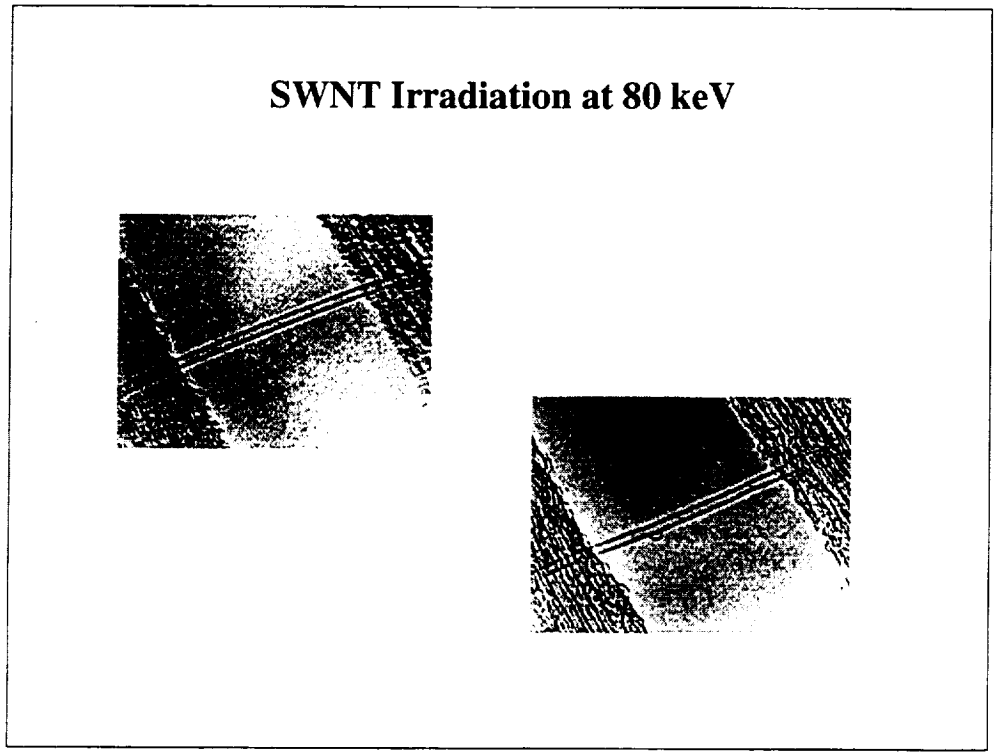

## SWNT Irradiation at 100 keV

At 100 keV, the top and bottom of the nanotube is damaged with the side walls remaining intact as can be seen from the strong continuous contrast. The loss of top and bottom surfaces is detectable by the lack of parallel registry between the two side walls.

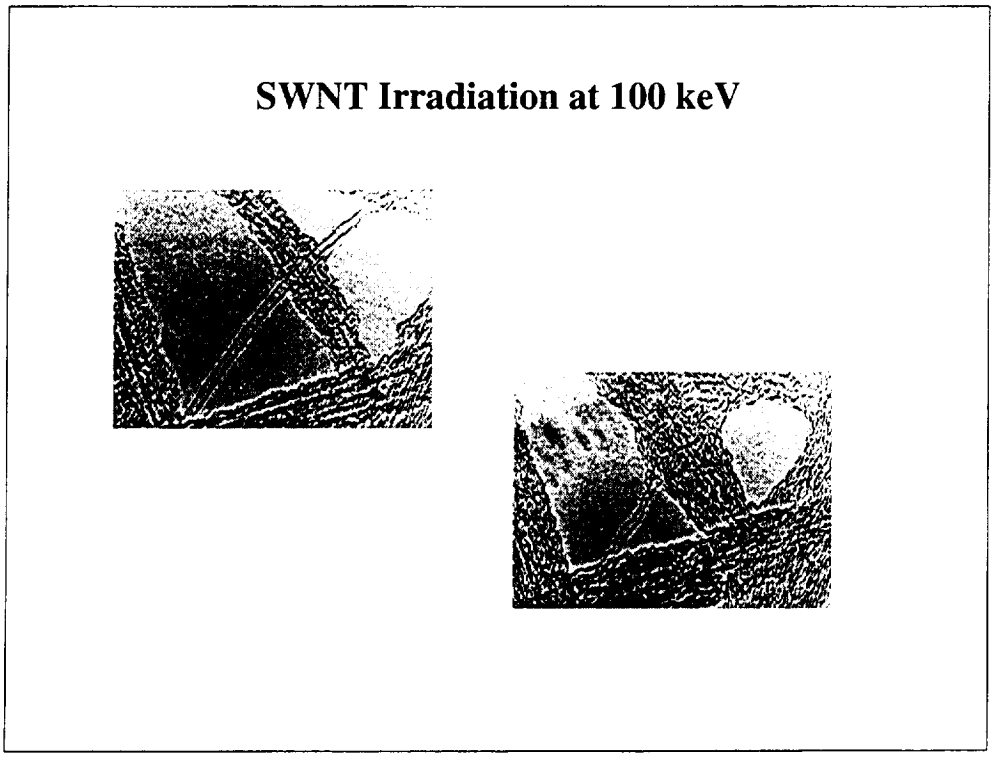

## SWNT Irradiation at 200 keV

At 200 keV, the nanotube is amorphized with all surfaces destroyed.

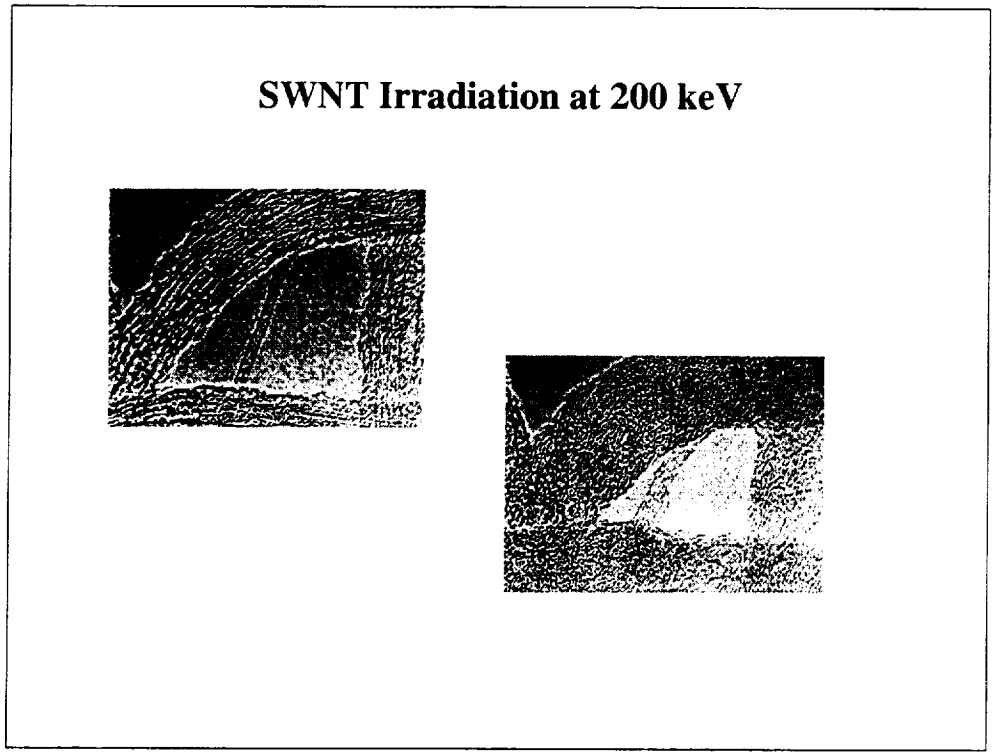

**Functionalized Nanotubes**

There are three possible paths to SWCNT functionalization: clockwise from upper left – attachment of side groups to the nanotube walls and ends; intercalation of the interstices in the SWCNT lattice; and intracalation of molecules within the lumen of the SWNCT. Schematics from the Smalley group (Rice), the Fischer group (UPenn), the Luzzi group (UPenn).

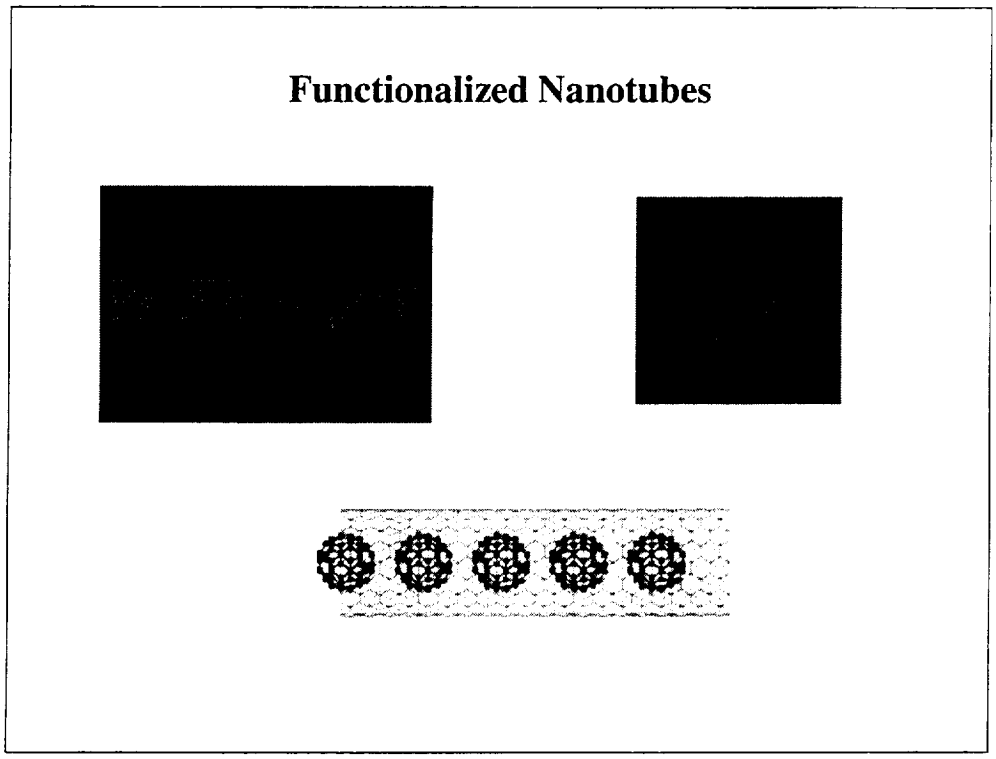

## Empty and Filled SWNTs

High magnification TEM micrographs of an empty SWCNT and a SWCNT filled with a linear chain of $C_{60}$ molecules. The scale bar is 2 nm.

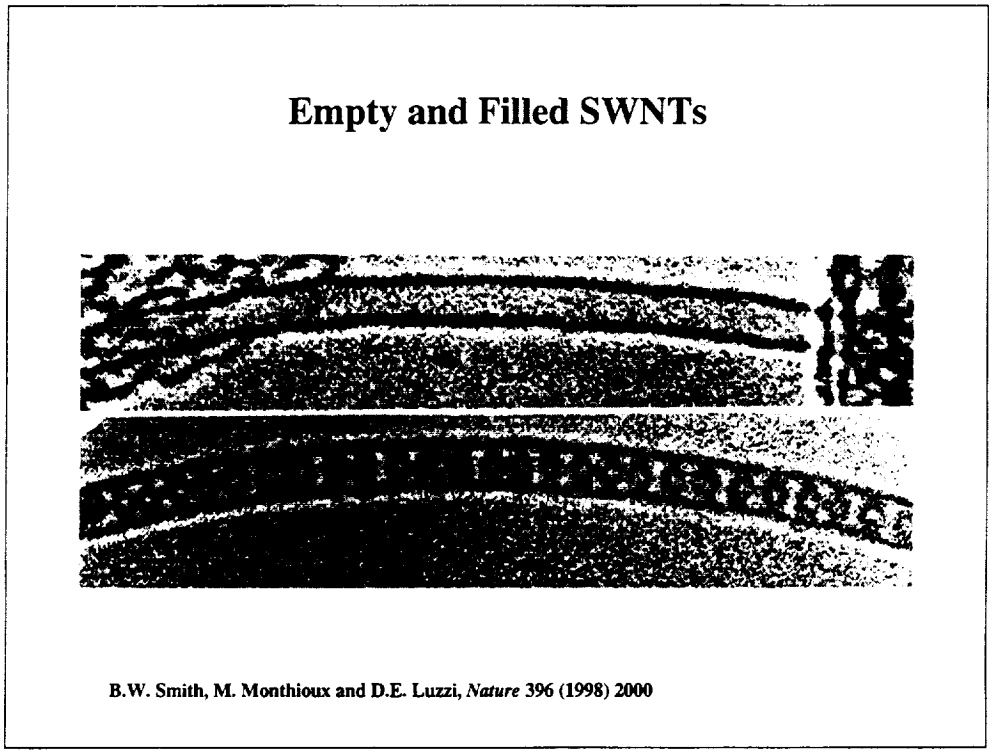

Schematic of the structure of a linear chain of $C_{60}$ molecules within an SWCNT.

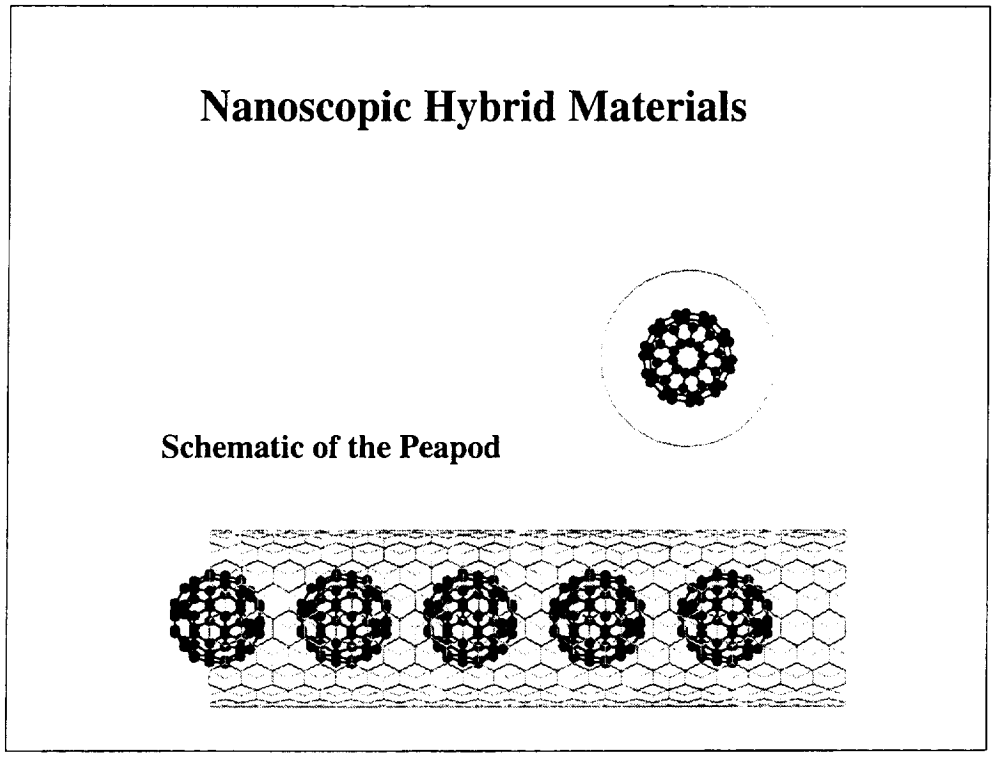

## Detection of $C_{60}$ Liberated From Peapods

Early UV-VIS experimental results used to prove that the interior molecules of the peapod were indeed $C_{60}$. This experiment also provided the first indication that molecules could be extracted from the inside of an SWCNT.

### Detection of $C_{60}$ Liberated From Peapods

- **PLV/Purified/Annealed Material Containing Peapods**
- **UV-VIS Spectroscopy (Control)**
- **Strong Acid Etch $H_2SO_4$ (90%):$HNO_3$ (70%) (3:1)**
  - 90 °C, 10 min
- **UV-VIS Spectroscopy**

| Sample | Mass Loss | $C_{60}$ Mass Fraction | $C_{60}$ Mole Fraction | Filled SWNT Mass Fraction |
|---|---|---|---|---|
| Etch-1 | 0.857 | 0.0974 | 0.0087 ±0.0001 | 0.023 |
| Etch-2 | 1.1 | 0.0175 | 0.016 ±0.003 | 0.030 |
| Etch-3 | 1.45 | 0.0297 | 0.0205 ±0.0003 | 0.054 |
| Control | 1 | undetected | <0.00008 | <0.0004 |

B. Burteaux, A. Claye, B.W. Smith, M. Monthioux, D.E. Luzzi, J.E. Fischer, *Chem. Phys. Lett.*, 310 (1999) 21.

## Formulation of Peapods in PLV Material

Upper left – as-received PLV material that has been acid purified and is coated with surrfactant. Upper right – the same material (not same location) after removal of the surrfactant; the acid-damaged nanotubes can be seen (as shown earlier).

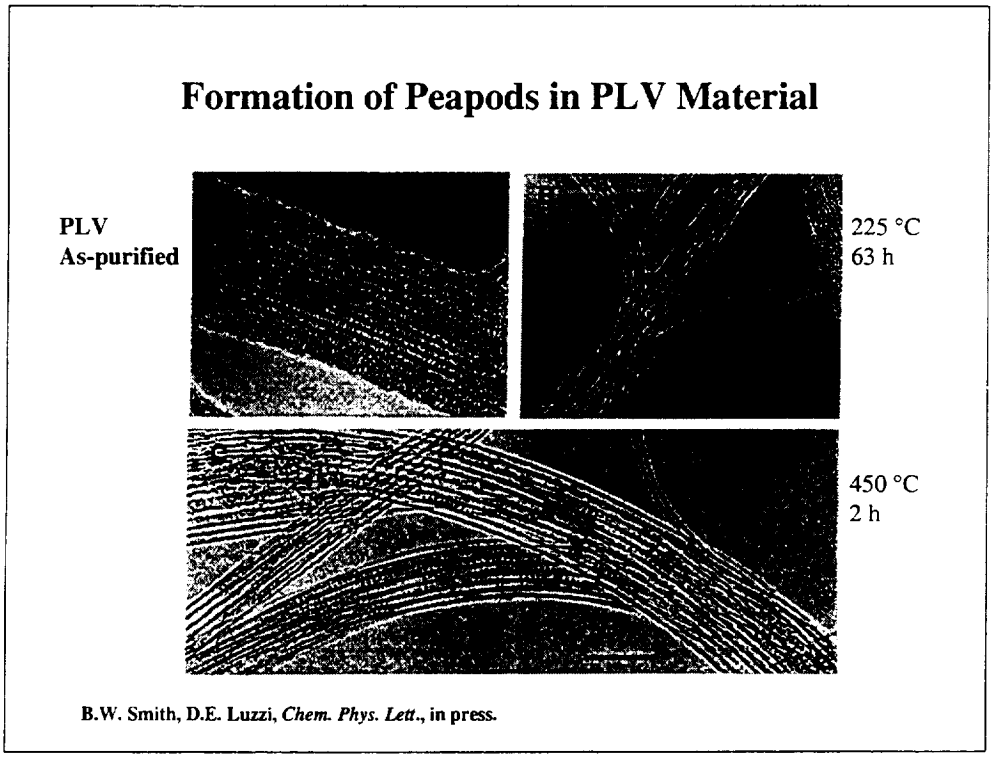

**In-Situ Anneal - 350 °C**
**Low Temperature Onset > 325 °C**

At temperatures above 325 °C in high vacuum, residual $C_{60}$ within the sample becomes mobile and comes into contact with nanotube exterior walls.

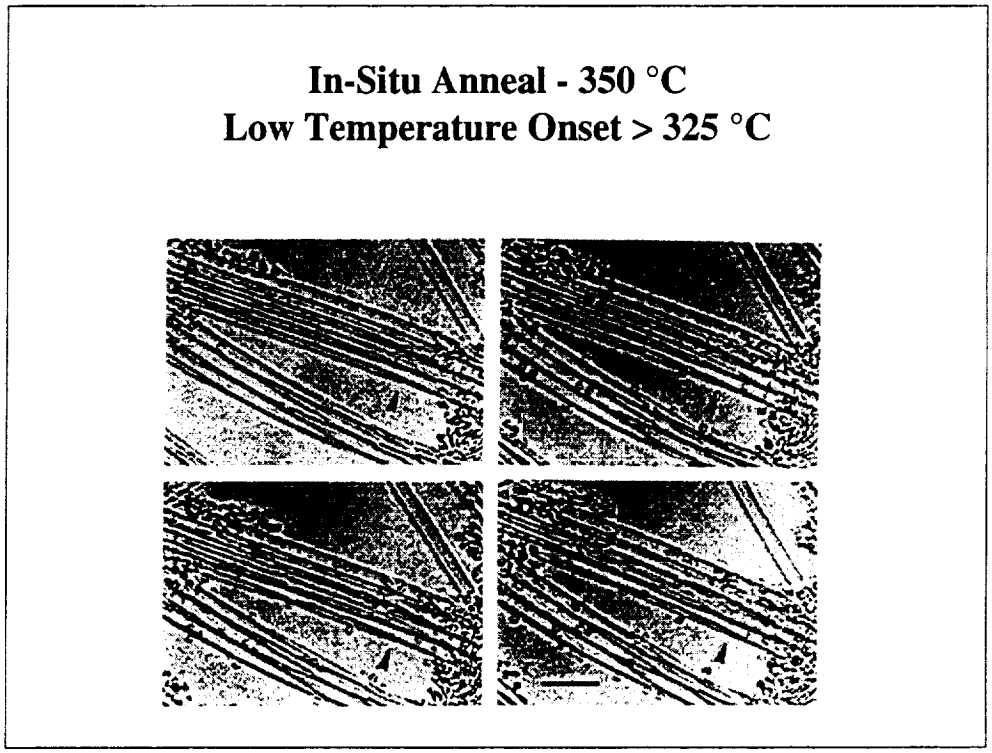

## Formation of Peapods in PLV Material

Bottom figure – $C_{60}$ then enters the nanotubes forming 1-D chains.

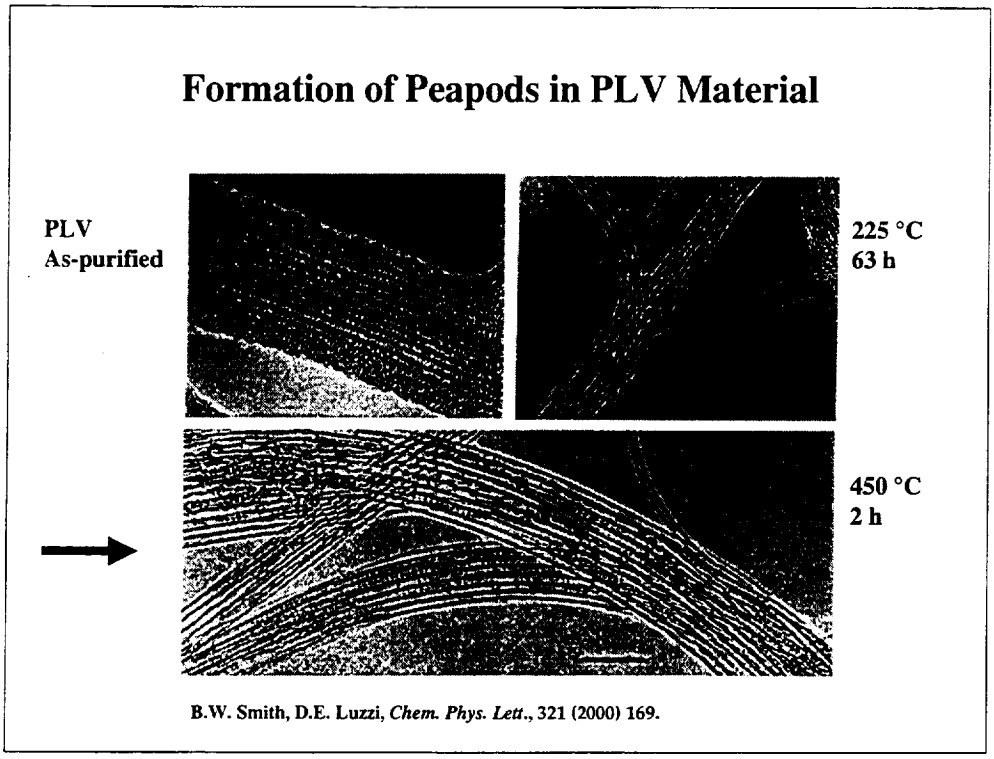

## CA Material (Peapod Specimen) - 400 °C, 1 h

Filling is possible at high efficiency and in nanotubes produced by different methods. This SWCNT material was produced using the CA method. $C_{60}$ was added to the material from a solution.

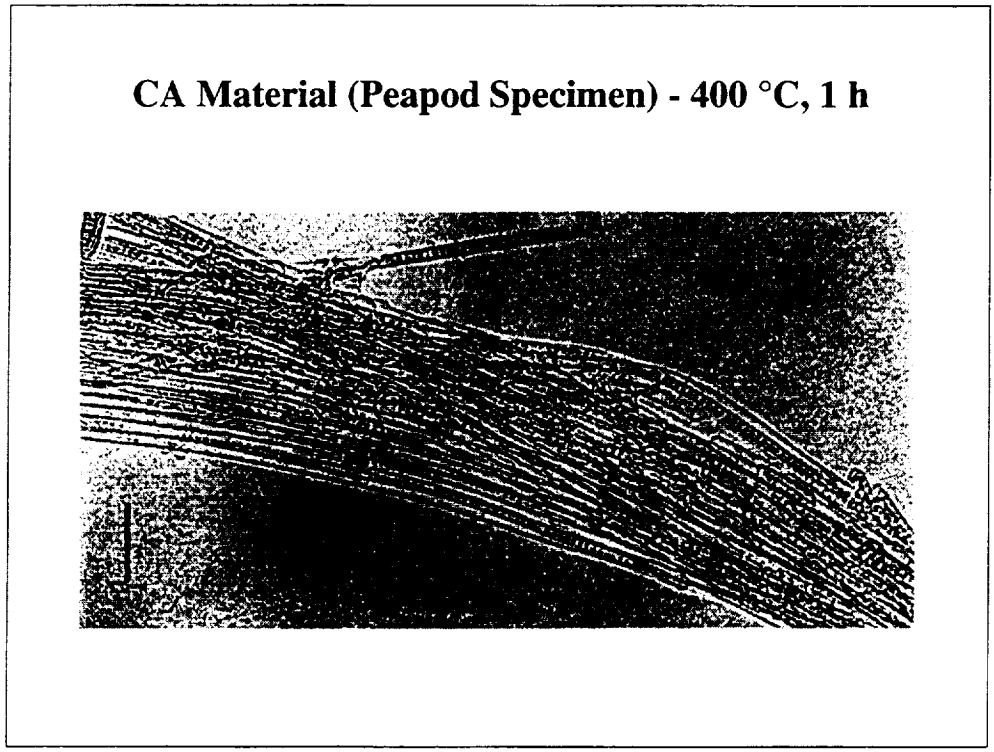

**Disordered $C_{60}$ Filling a 2.7 nm Nanotube**
**CA Material - 400 °C, 1 hour**

Image of a disordered cluster of $C_{60}$ filling a large diameter SWCNT. Scale bar is 5 nm. This provides important evidence that nanotubes can be filled with molecules, even when the size of the molecules does not match the diameter of the nanotube lumen.

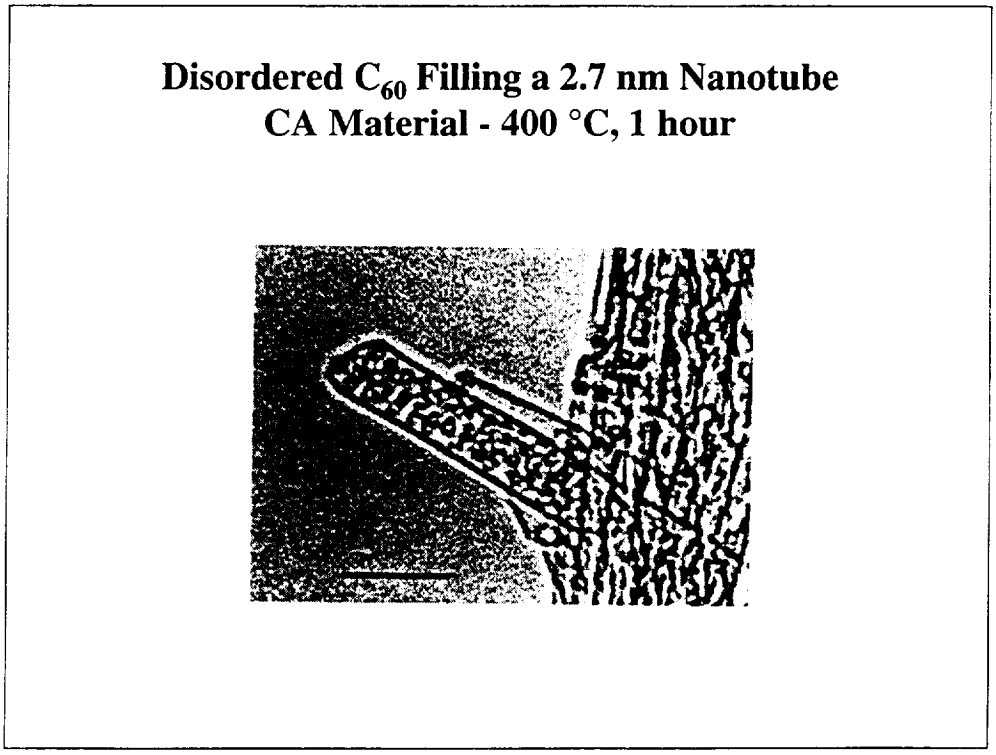

## Fullerene Motion - 100 keV

$C_{60}$'s can be induced to move within the SWCNT through interactions with the electron beam. This is a time sequence of the same cluster of five molecules with approximately 20s between images. Controlled mass transport along the lumen of nanotubes opens the possibility for a number of enabling nanotechnology applications.

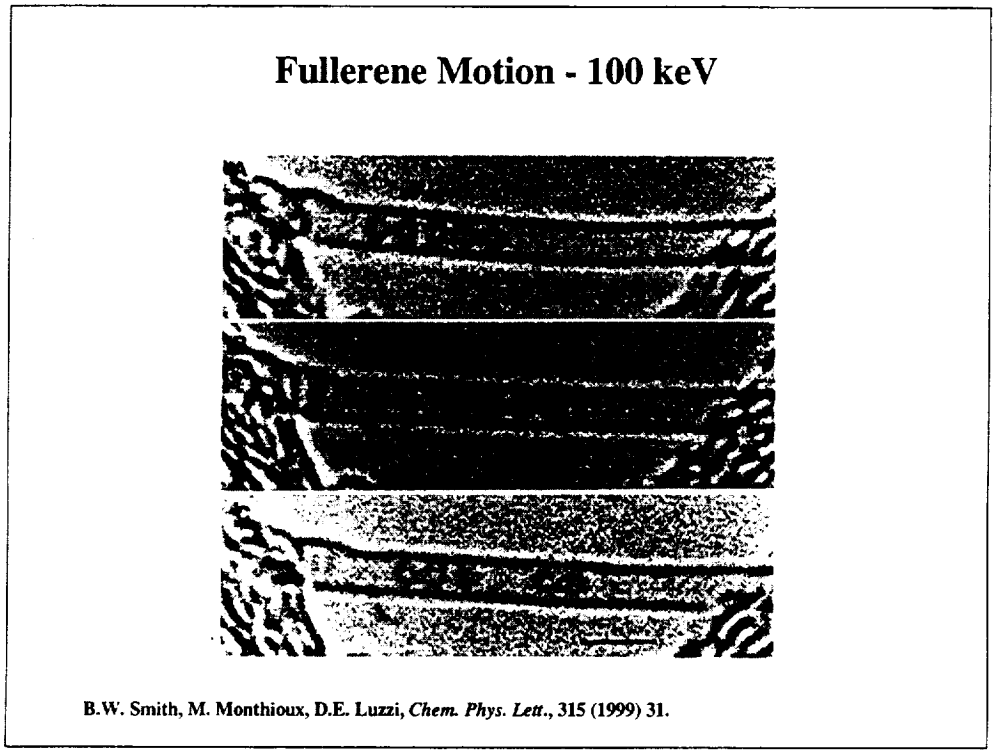

## $La_2@C_{80}$ - Motion of Individual Atoms

A TEM image of a 1-D chain of endohedral metallofullerene$La_2@C_{80}$ molecules within a 1.4 nm diameter SWCNT. This is a single frame of an in-situ video, so shot noise is present. However, the two La atoms can be seen as dark spots within the circles which are the $C_{80}$ cage.

Go to slide show view, move your mouse cursor over the image until a picture of a pointing finger appears and click. The video will show the tumbling motion of the two La atoms within the $C_{80}$ cages. These images were recorded at temperatures near room temperature.

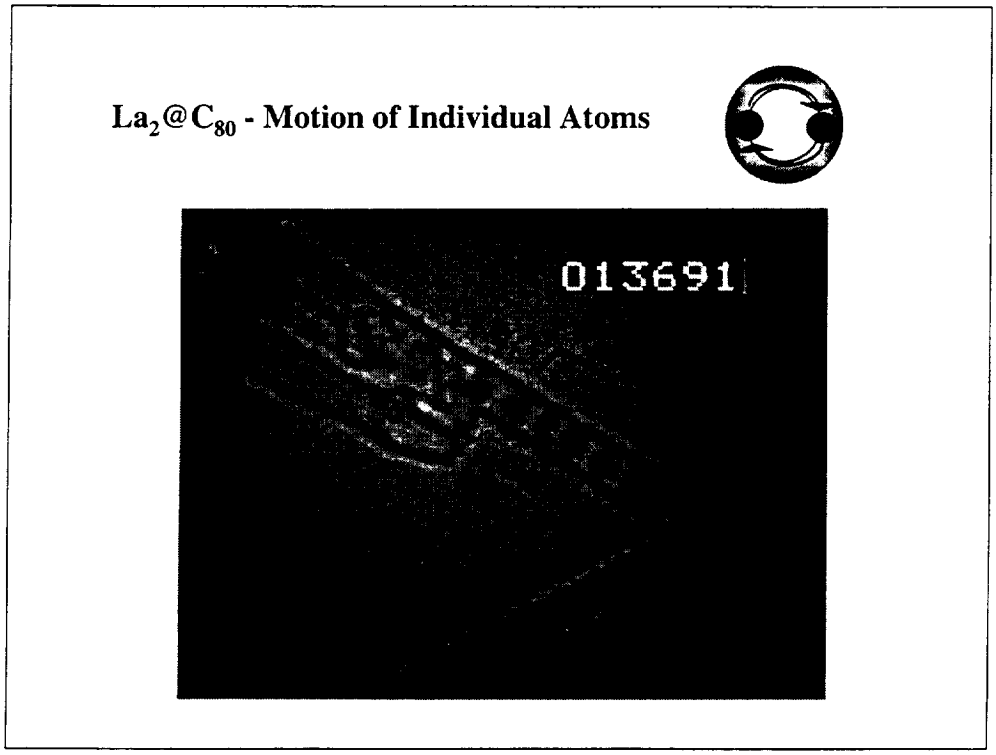

## Mechanical Response of (15.0) SWNT w/$C_{60}$

When a nanotube is deformed in tension, the extension of the nanotube induces a Poisson contraction that reduces its diameter. If the interior of the nanotube is filled with molecules such as $C_{60}$, the molecules will resist this compression and therefore increase the stiffness of the nanotube. This is seen in this atomistic simulation that shows a slope change in the strain energy versus tensile strain curve at the point at which the interior $C_{60}$'s begin to undergo compressive deformation. Thus, it is expected that the hybrid nanotubes containing $C_{60}$ will be stiffer than the nanotube alone, which is already the stiffest material known.

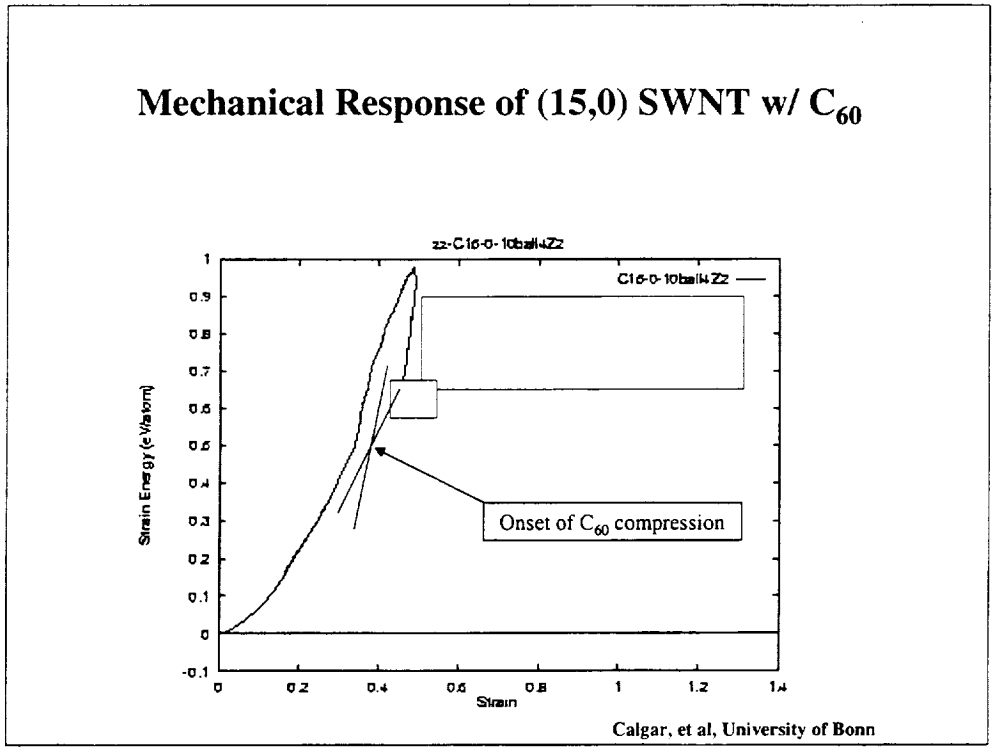

## Chemistry in Confined Environments

When the hybrid nanotube containing $C_{60}$ is heated to high temperatures, the $C_{60}$ molecules coalesce into interior cylindrical capsules and tubes. These capsules are mobile within the nanotube indicating that no reaction occurs between the nanotube and the interior molecules. Thus, the nanotube provides two functions: it catalyzes the reaction by confining the reactants in close proximity and, controls the structure of the reaction product through steric confinement. A clear example is the indicated capsule of $C_{180}$. The equilibrium structure of this molecule is more spherical. Within the nanotube, it is restricted to form this cylindrical form, which is a metastable configuration.

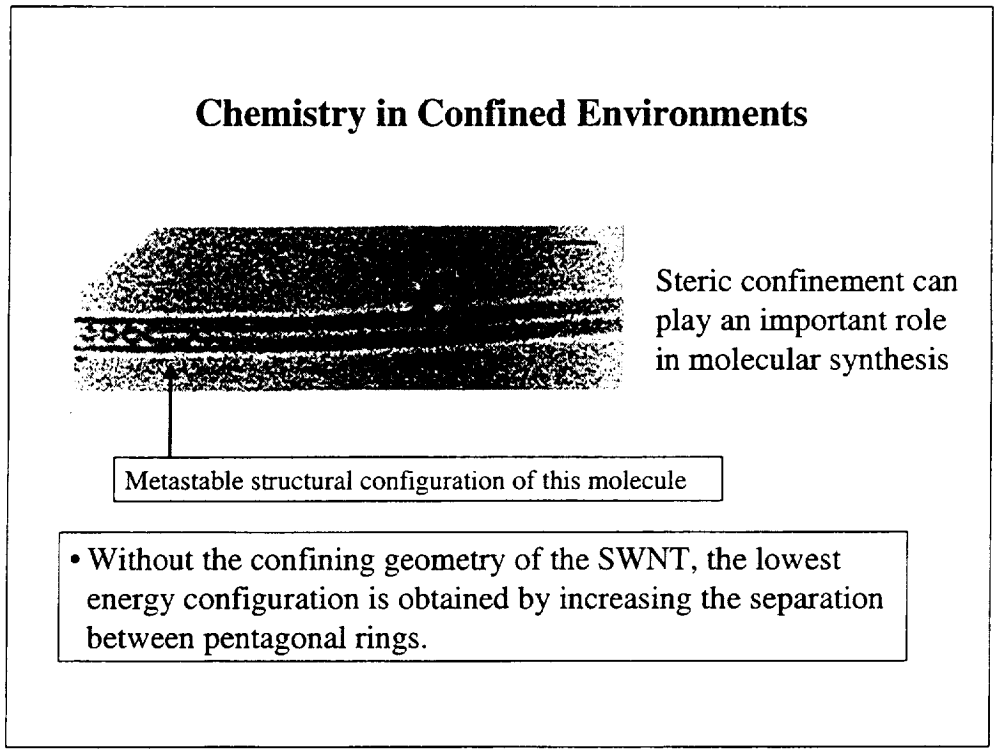

## Nanometer-sized Furnace Tubes

In order to carry out useful chemistry in nanometer-sized reaction vessels, one must be able to carry out three tasks listed below in yellow. In the present work, each of these concepts has been developed. It remains to be tested whether nanotube-based synthesis can be used on a bulk scale.

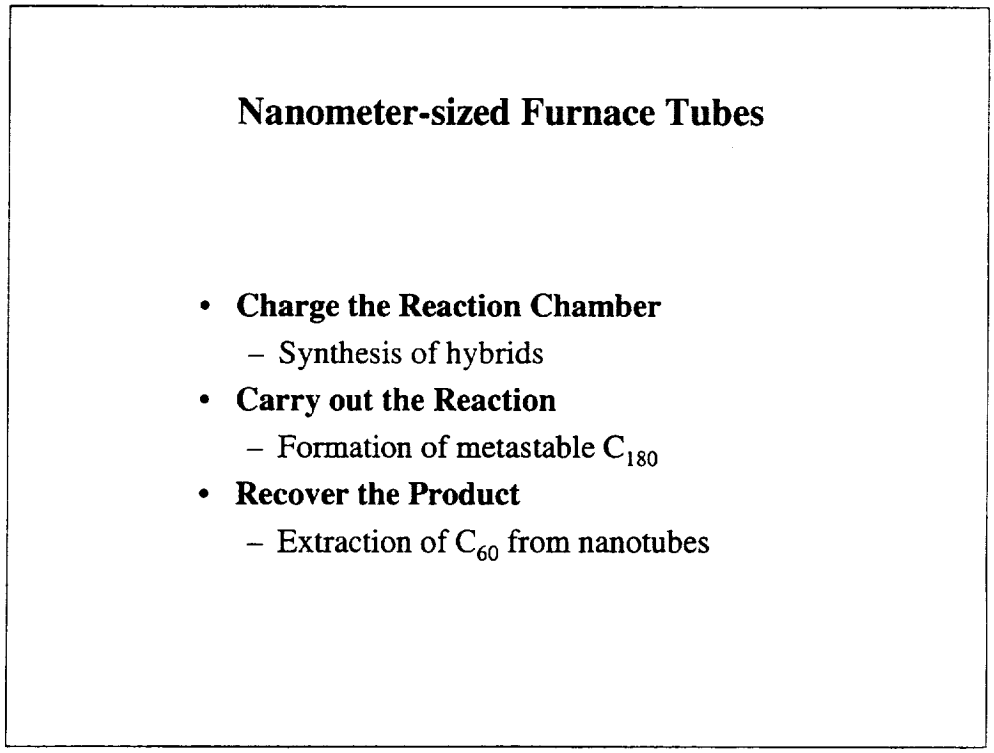

## Improved Stiffness of Small SWNT's

Both ab-initio and statics calculations have shown that the stiffness of nanotubes in bending will increase with decreasing diameter. Thus, the production of small tubes within the larger nanotubes from the $C_{60}$-nanotube hybrid should yield a stiffer nanotube, but without significant changes to other nanotube properties, such as the chemical reactivity.

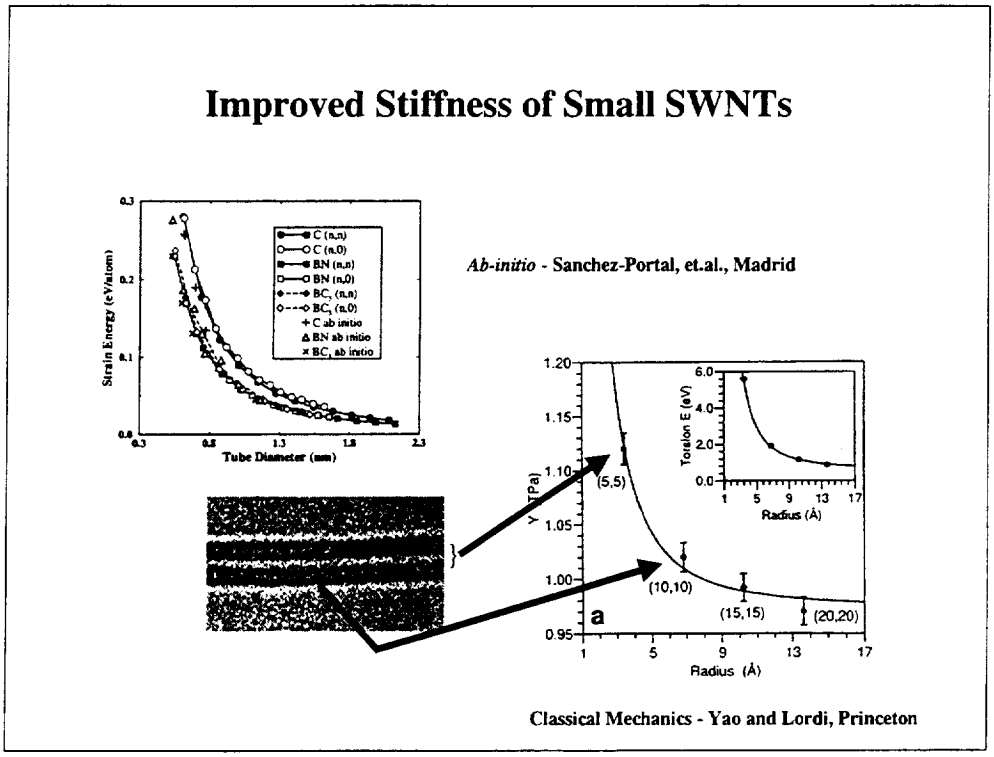

## Using SWNTs for the Study of Single Molecules

The work has also demonstrated the efficacy of nanotubes as substrates for the study of individual molecules. It has been extraordinarily difficult to study single molecules due to the problems posed by background signals from substrates. Nanotubes provide a stable, radiation damage resistant (at low voltages), extremely high observation area substrate.

### Using SWNTs for the Study of Single Molecules

7 Angstroms!

Any molecule that will enter a SWNT or bind/physisorb to the exterior of a nanotube can be studied by imaging, diffraction or spectroscopy

We are imaging stable single molecules at close to atomic resolution without effort!

## Acknowledgments

Smith and Monthioux at Penn (MM permanent address: CEMES, Toulouse, France)

Nanotube materials (pre-filling) graciously provided by Rice, Montpellier and CNRS Strasbourg.

Funding from NSF and ONR.